

# Automatika

Journal for Control, Measurement, Electronics, Computing and Communications



ISSN: (Print) (Online) Journal homepage: [www.tandfonline.com/journals/taut20](http://www.tandfonline.com/journals/taut20)

## Stratifying transformer defects through modelling and simulation of thermal decomposition of insulating mineral oil

A. Manjula, Sangeetha S, Mustafa Musa Jaber, Hamad Mohamad A.A, Santosh Kumar Sahu, Rajesh Verma & Prashant Vats

To cite this article: A. Manjula, Sangeetha S, Mustafa Musa Jaber, Hamad Mohamad A.A, Santosh Kumar Sahu, Rajesh Verma & Prashant Vats (2023) Stratifying transformer defects through modelling and simulation of thermal decomposition of insulating mineral oil, *Automatika*, 64:4, 733-747, DOI: [10.1080/00051144.2023.2197821](https://doi.org/10.1080/00051144.2023.2197821)

To link to this article: <https://doi.org/10.1080/00051144.2023.2197821>



© 2023 The Author(s). Published by Informa UK Limited, trading as Taylor & Francis Group



Published online: 24 May 2023.



Submit your article to this journal [↗](#)



Article views: 614



View related articles [↗](#)



View Crossmark data [↗](#)



Citing articles: 3 View citing articles [↗](#)



# Stratifying transformer defects through modelling and simulation of thermal decomposition of insulating mineral oil

A. Manjula<sup>a</sup>, Sangeetha S<sup>b</sup>, Mustafa Musa Jaber<sup>c</sup>, Hamad Mohamad A.A.<sup>d,e</sup>, Santosh Kumar Sahu<sup>f</sup>, Rajesh Verma<sup>g</sup> and Prashant Vats<sup>h</sup>

<sup>a</sup>Department of Electrical and Electronics Engineering, Mohamed Sathak Engineering College, Kilakarai, India; <sup>b</sup>Department of Marine Engineering, AMET University, Chennai, India; <sup>c</sup>Department of Medical instruments engineering techniques, Al-Farahidi University, Baghdad, Iraq; <sup>d</sup>Department of Physics, College of Education, Samarra University, Iraq; <sup>e</sup>Department of Medical instruments engineering techniques, Dijlah University College, Baghdad, Iraq; <sup>f</sup>Department of Mechanical Engineering, Veer Surendra Sai University of Technology, Burla, India; <sup>g</sup>Department of Electrical Engineering, College of Engineering, King Khalid University, Abha, Kingdom of Saudi Arabia; <sup>h</sup>Department of CSE, SCSE, Manipal University Jaipur, Jaipur, Rajasthan, India

## ABSTRACT

The current work aims to propose an adequate thermodynamic model, in addition to proposing and evaluating two composite models for the thermal decomposition of insulating mineral oil (IMO), considering that the models based on classical diagnostic methods do not have the ability to satisfactorily reproduce empirical data. The simulation results obtained using the proposed model showed better agreement with the presented data than the results obtained using classical models. The proposed model was also used in the development of a phenomenological based diagnostic method. The characteristics of this new phenomenological proposal and the classical diagnostic methods of dissolved gas analysis are compared and discussed; the proposed method showed better performance when compared to Rogers, Doernenburg, or IEC and equivalent performance to Duval triangle method commonly used in this field of knowledge. The general procedure for applying the new diagnostic method is also described. In order to account for the event's dynamics, the suggested model in particular made it feasible to replicate intermediate scenes of equilibrium C(s). Compared to the findings from the classical models found in the literature, the two-dimensional simulation results generated with this model demonstrated a better agreement with the actual data.

## ARTICLE HISTORY

Received 12 January 2022  
Accepted 28 March 2023

## KEYWORDS

Dissolved gas; Insulating mineral oil; incipient defects; Sum of squares of the relative residuals

## 1. Introduction

Insulating mineral oil (IMO) is a petroleum derivative widely used in high voltage power transformers, especially in power transmission system devices. Due to the relevance of power transformers to the electrical system and the risks and high costs involved in their malfunction, predictive maintenance techniques have been developed and improved over the last 80 years [1–5]. These techniques aim to detect defects in power transformers. The best known of these predictive maintenance techniques is dissolved gas analysis (DGA). The DGA technique consists of collecting IMO samples from equipment in operation and quantifying the concentrations of some specific light compounds (gases) that are produced by the cracking of IMO molecules and remain dissolved in the liquid phase. The set formed by the concentrations of these light compounds is then used to verify the existence of a defect and, also, to classify this defect through semi-empirical algorithms, known as diagnostic methods.

This correlation between concentrations of dissolved gases in IMO and types of defects in transformers is possible, since the energy dissipated to the oil in the vicinity of a defective region implies a local temperature and, therefore, determines which products will be predominant in the equilibrium of the reaction of consequent cracking [6]. The sensitivity of dissolved gas analysis makes it possible to identify defects that are still incipient, difficult to detect using other predictive techniques.

The effectiveness of dissolved gas analysis is, admittedly, a well-established and consolidated issue. However, despite the importance of this technique, widely known and applied DGA diagnostic methods, such as the classic methods of the International Electrotechnical Commission (IEC) and the Institute of Electrical and Electronics Engineers (IEEE), are theoretically based on the Halstead's simplistic compositional and thermodynamic models for the thermal decomposition of the IMO, in addition to empirical data.

**CONTACT** Sangeetha S  sebastianvindrojude@gmail.com  Department of Marine Engineering, AMET University, Chennai 600 119, Tamil Nadu, India

This article has been corrected with minor changes. These changes do not impact the academic content of the article.

© 2023 The Author(s). Published by Informa UK Limited, trading as Taylor & Francis Group

This is an Open Access article distributed under the terms of the Creative Commons Attribution License (<http://creativecommons.org/licenses/by/4.0/>), which permits unrestricted use, distribution, and reproduction in any medium, provided the original work is properly cited. The terms on which this article has been published allow the posting of the Accepted Manuscript in a repository by the author(s) or with their consent.

Recently, most research efforts in DGA have been devoted to the development and improvement of so-called intelligent diagnostic methods and numerous articles on the topic have been published over the years [7–16]. Smart methods attempt to improve the performance of classic diagnostic methods, either by combining the responses of two or more classic methods or by establishing new diagnostic criteria based on empirical data and/or tacit knowledge of the maintenance specialist. Also recently, new diagnostic methods have been developed based on the proposal to evaluate new sets of normalized ratios or fractions of dissolved gases [17,18]. Therefore, the Halstead model and empirical data remain the fundamental basis of DGA, even for the latest and most intelligent diagnostic methods. No recent effort for the development of thermodynamic and compositional models more suitable to represent the thermal decomposition of the IMO could be identified in the technical literature.

The present work aims to propose a more adequate thermodynamic modelling, in addition to proposing and evaluating four compositional models for the thermal decomposition of the IMO, considering that the models on which the classical diagnostic methods are based are not able to satisfactorily reproduce the empirical data [19,20]. In addition, a new diagnostic method by DGA is presented, with a phenomenological basis, developed from the proposed thermodynamic and compositional models. Finally, the performance of the new diagnostic method is evaluated and a comparison with the classical diagnostic methods of the IEC and the IEEE is conducted [21–25].

Despite being the greatest alternative to mineral oil, vegetable oil has a number of drawbacks, such as a high dielectric loss factor, poor volume resistivity, and a high viscosity. Vegetable oil's electrical characteristics might be greatly enhanced via nanoparticle treatment. In this work,  $\text{Fe}_3\text{O}_4$ ,  $\text{TiO}_2$ , and  $\text{Al}_2\text{O}_3$  nanoparticle-infused vegetable oil was examined [26–30]. We conducted thermal ageing tests at 100, 130, and 150 °C. However this method is not stable when compared to the proposed method and correctness diagnostics achieved 80% in proposed method.

The flowchart of the proposed T-C method application procedure is shown in Figure 1.

### 1.1. Typical incipient defects

The IEC database consists of 117 sets of volumetric concentrations of dissolved gases in IMO of defective electrical equipment, each associated with a type of defect; this, in turn, assigned by specialists through internal visual inspection in the corresponding equipment. The types of defects can be divided, primarily, into two large classes: thermal defects and electrical defects. In the IEC database, the class of thermal defects has been

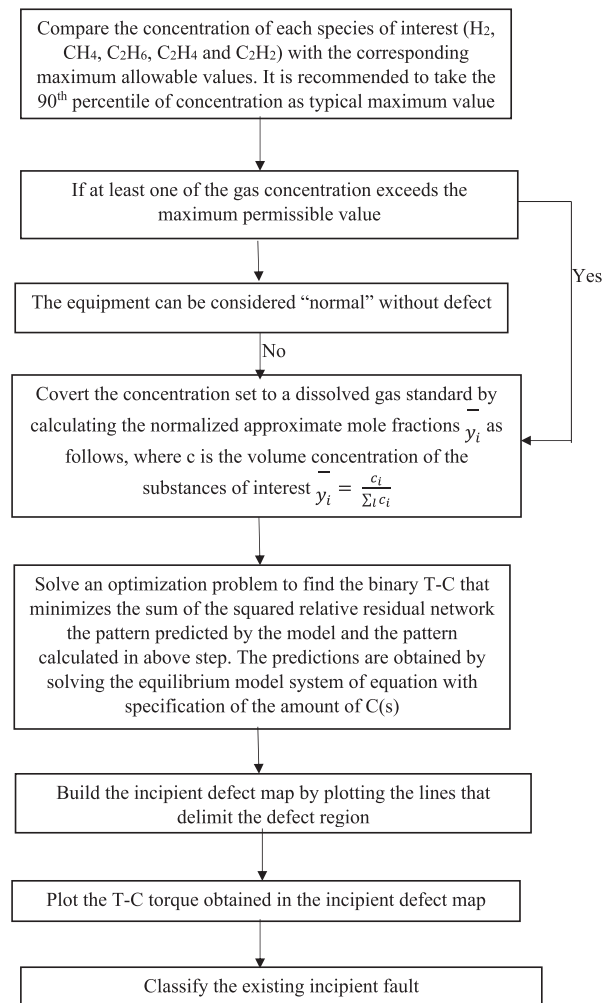


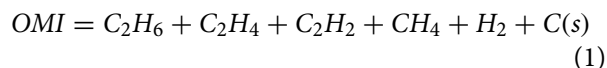
**Figure 1.** The flowchart of the proposed T-C method application procedure.

subdivided into two types of defects: low/medium temperature thermal defects and high temperature thermal defects [31,32]. The class of electrical defects was subdivided into three types of defects: partial discharges, low-energy electrical discharges and high-energy electrical discharges. In this paper, the same structure of classification of incipient defects was adopted. Assuming ideal gas behaviour for the mixture, for each reported case, the volumetric concentrations of the dissolved gases of interest for the diagnostic methods, produced by the decomposition of the IMO, that is,  $\text{C}_2\text{H}_6$ ,  $\text{C}_2\text{H}_4$ ,  $\text{C}_2\text{H}_2$ ,  $\text{CH}_4$  and  $\text{H}_2$ , were normalized in order to obtain the respective molar fractions. Then, the lower and upper limits of the confidence interval, for a 95% confidence level, were calculated for all species of interest in each incipient defect type.

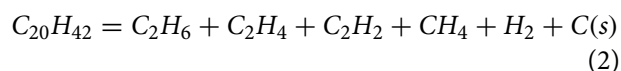
## 2. Compositional modeling

Four systems were proposed to represent the local structure of the IMO near the initial defect. Since the contents of the gases  $\text{C}_2\text{H}_6$ ,  $\text{C}_2\text{H}_4$ ,  $\text{C}_2\text{H}_2$ ,  $\text{CH}_4$  and  $\text{H}_2$

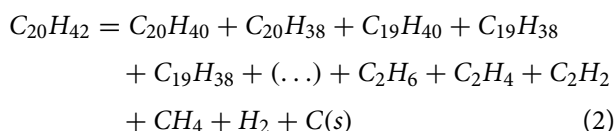
are commonly measured and used by classical diagnostic methods, the presence of these species in equilibrium systems was considered the minimum requirement for all proposed systems. Systems 1 consist of 6 and 7 species. Therefore, the equilibrium system is made up of light types that are most interested in detection methods, i.e.  $C_2H_6$ ,  $C_2H_4$ ,  $C_2H_2$ ,  $CH_4$  and  $H_2$  and  $C(s)$ . The characteristic decay reaction of system 1 can be described as follows:



In this system 2, all components of the unreacted IMO are represented by n-icosane, which is partially decomposed into lighter species. Unlike the aforementioned study, in the present work, the propane ( $C_3H_8$ ) and propene ( $C_3H_6$ ) species are suppressed, so that the decomposition of n-icosane results in only the light species of interest. The equilibrium system is composed of n-icosane, the light species of interest and  $C(s)$ . The characteristic decomposition reaction of System 2 is listed below:

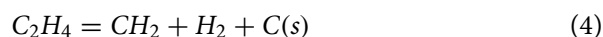
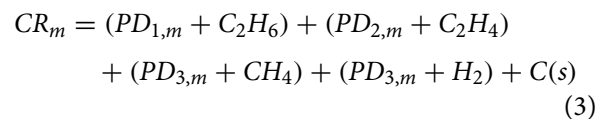


System 3 is an expanded version of System 2. n-icosane, again, represents all components of the unreacted IMO, however, when exposed to the local temperature of a defective region, its decomposition leads to complete series of alkanes, 1- linear alkenes and 1-alkynes, whose carbon chain sizes vary from 1 to 20 carbons. The equilibrium system consists of 60 species, namely: 20 alkanes, 19 1-alkenes, 19 1-alkynes,  $H_2$  and  $C(s)$ . The decomposition reaction is shown below.



System 4 assigns 1 representative component to each of the 15 families of hydrocarbons reported in [32]. Non-hydrocarbon families have been deleted. The decomposition of these representative components leads to the same 5 light species of interest present in the previous systems and 60 more by-products, in addition to  $C(s)$ . It is assumed that the process takes place in two steps: in the first step, the paraffinic chain of each representative component decomposes into  $C_2H_6$ ,  $C_2H_4$ ,  $CH_4$ ,  $H_2$  and  $C(s)$  and, in the second step,  $C_2H_4$  decomposes into  $C_2H_2$ ,  $H_2$  and  $C(s)$ . The equilibrium system, therefore, consists of 81 species: 15 representative components of the unreacted IMO hydrocarbon families, 60 decomposition by-products, in addition to the species of interest  $C_2H_6$ ,  $C_2H_4$ ,  $C_2H_2$ ,  $CH_4$  and  $H_2$  and  $C(s)$ . The decomposition scheme proposed in System 4 can be represented by the following reactions, where CR

corresponds to a representative component, PD represents a matrix of decomposition by-products and the subscript m is an index that identifies each representative component:



### 3. Numerical optimization

In order to allow the qualitative and quantitative evaluation of the obtained simulation results, 117 optimization problems were solved to compare each one of the patterns of dissolved gases from the IEC database with the patterns from the simulations with each variation of the proposed model of decomposition of the IMO. The objective of such optimization problems was to find the optimal parameters that would lead to the minimization of the sum of squares of the relative residuals between the predicted molar fractions and the molar fractions coming from the IEC database. As the mentioned objective function does not admit empirical molar fractions equal to zero, in such cases, the lower detection limit of each gas was adopted, according to interlaboratory studies conducted by ASTM International.

The molar fraction matrices predicted in the scenarios of unrestricted amounts of  $C(s)$  and without  $C(s)$  gave rise to one-dimensional optimization problems, whose parameter is the temperature. On the other hand, the molar fraction hypermatrices predicted in the scenario of optimized amount of  $C(s)$  gave rise to two-dimensional optimization problems, whose parameters are the temperature and the fraction of the unrestricted amount of  $C(s)$  equilibrium.

The mentioned objective function corresponds to Equation (3.1), where SOS means sum of squares of relative residuals and  $y$  is the molar fraction. The subscript l is an index that identifies each of the five species of interest, the subscript IEC refers to the IEC database, and the subscript "pred" refers to the data predicted by the decomposition model. Figure 2 presents the structures of the one-dimensional and two-dimensional optimization algorithm.

$$SOS = \sum_l \left( \frac{y_l - y_{l,pred}}{y_l} \right)^2 \quad (5)$$

A brute force approach was used to solve these problems, thus exploring the full range of interest for both the temperature and the uncontrolled equilibrium level of  $C(s)$ , thus avoiding errors related to local minima. According to Equation (4), the MRE was calculated as the percentage mean error corresponding to the

optimal values of the objective function [26–31]. And “otm” refers to the optimal value.

$$MRE = 100 \sqrt{\frac{SOS_{otm}}{5}} \quad (6)$$

#### 4. Development of The T-C Diagnostic Method

The simulation results obtained from the IMO heat dissipation model were used to improve the C(s) magnitude and to ethane develop a diagnostic method based on T-C systematic phenomena. The equilibrium temperature and the uncontrolled equilibrium area of the C(s) parameters will be used to relate the sample predictions to the empirical data of the dissolved gases. The method followed for the development of the method is described below.

##### 4.1. Defect maps

The results obtained in the solution of the 117 two-dimensional optimization problems, referring to the OMI thermal decomposition model composed by the System 3 compositional model and by the thermodynamic model with specification of the amount of C(s). The results of the optimization problems used here refer to the hypermatrix of predicted molar fractions of dimensions  $2001 \times 101 \times 5$ , that is, the one obtained in simulations with increments of 0.01 in the fraction of the unconstrained equilibrium quantity of C(s). The optimal pairs of equilibrium temperature, T, and fraction of the unrestricted equilibrium quantity of C(s), C, obtained as solutions to the optimization problems, here called T-C binaries, were plotted on a C vs T graph. Then, regions of incipient defects were delimited through visual inspection, aiming to maximize the number of correct allocations of defects in the corresponding regions on the map. In a first step, the map of incipient defects was divided into three regions, each characterizing a class of incipient defects, namely: (i) partial discharges (DP), (ii) thermal defects (DT) and (iii) electrical discharges (DE). Then, the map was divided into five regions, in order to allow a complete representation of the incipient defects listed in the IEC database, namely: (i) partial discharges (PD), (ii) low/medium temperature thermal defects (T1/T2), (iii) high temperature thermal defects (T3), (iv) low energy electrical discharges (D1) and (v) high energy electrical discharges (D2). The proposed method consists of classifying the incipient defect associated with a given set of dissolved gas concentrations, through its allocation in a region of the three-region map or the five-region map in the C vs T diagram.

##### 4.2. T-C method performance analysis

The 117 sets of dissolved gas concentrations from the IEC database were detected in both the T-C method and

the classical method. The selected criterion for evaluating performance is the percentage of accurate diagnoses obtained from the use of each method.

Two performance assessments were conducted: the first evaluated the ability to classify the initial defects of each method as PD, TD or ED and the second evaluated the classification as PD, T<sub>1</sub>/T<sub>2</sub>, T<sub>3</sub>, D<sub>1</sub> and D<sub>2</sub>.

Classification into three defects and five defects required some adjustments to guarantee the quality of the answers of the different evaluation methods. In cases where the response of a method is equivalent to many of the classifications listed in the previous paragraph, the diagnosis is considered conservatively correct if at least one of the classifications provided by the method matches the visual classification reported in the IEC database. Similarly, in cases where the initial defect is associated with multiple visual classifications, the diagnosis is considered correct if the response of the method corresponds to at least one of these visual classifications.

Due to the limited size of the IEC database, the dissolved gas datasets used in the performance appraisal of the T-C method were used in its development. However, the database was randomly divided into two independent subgroups to determine the limits of the defective areas and to evaluate the performance of the system, and these gave visually equivalent results without dividing the database.

## 5. Results and discussion

The results are divided into central aspects of the problem, namely: simulation and optimization and the T-C diagnostic method.

### 5.1. Simulation and optimization results

This section considers the results obtained in the chemical equation simulations and the solution of the optimization problems according to the methods described above.

### 5.2. Equilibrium molar fractions as a function of temperature

The results obtained in the simulations with the unrestricted thermodynamic model are presented as in Figure 6, in the form of profiles of molar fractions as a function of equilibrium temperature for Systems 1–4, respectively. In order to facilitate comparison with the typical patterns of incipient defects, the graphs are limited to presenting the normalized equilibrium molar fractions of the species of interest for the diagnostic methods by analysis of dissolved gases, ie, H<sub>2</sub>, CH<sub>4</sub>, C<sub>2</sub>H<sub>6</sub>, C<sub>2</sub>H<sub>4</sub> and C<sub>2</sub>H<sub>2</sub>. Each figure presents the simulation results for the two scenarios of

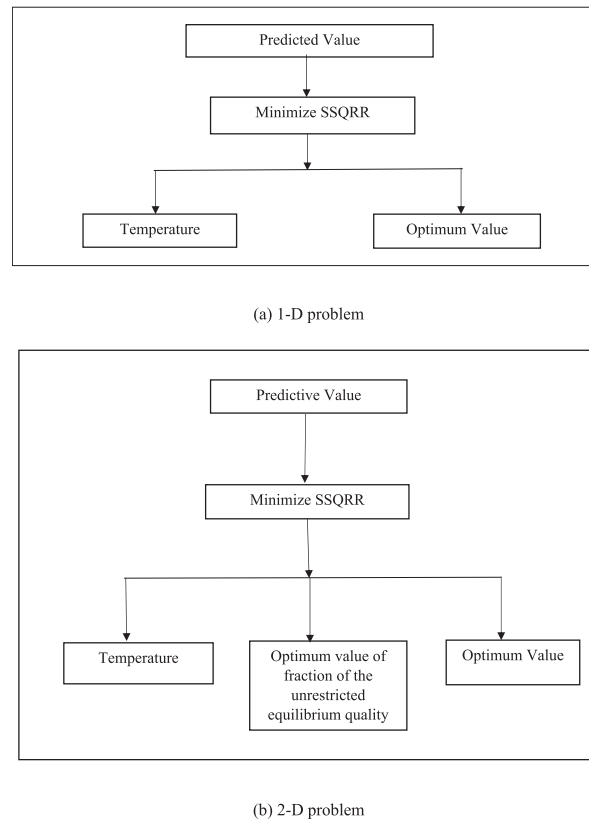


**Figure 2.** Optimization structures. (a) 1-D problem; (b) 2-D problem.

quantity of C(s) proposed in the literature: (i) scenario with unrestricted quantity of C(s) and (ii) scenario without C(s).

Analyzing Figure 3(a), Figure 4(1), Figure 5(a) and Figure 6(a), it is observed that the results of the simulations with unrestricted amount of C(s) are practically the same for the four systems, independently of the different compositional modelling of the OMI and the presence of heavier species. Furthermore, the comparison of these same figures with the typical patterns of incipient defects reveals that the proposed systems are not able to represent the OMI decomposition when an unrestricted amount of equilibrium of C(s) is admitted: while the simulation results present, virtually, only the hydrogen and methane species in the systems in equilibrium, as the results of the study by Halstead (6), the typical patterns show significant contents of all species of interest. Such findings are in agreement with the observations of Shirai et al. (23).

On the other hand, when comparing the typical patterns of incipient defects with Figures 3(b)–6(b), it is immediately observed that the proposed systems have the potential to represent the decomposition of the IMO when there are no C(s) in the equilibrium system, considering that the simulation results, this time, present significant amounts of other gases of interest, in addition to hydrogen and methane. However, the hypothesis of total absence of C(s) in equilibrium systems contradicts the empirical observations.

Systems 2 and 3, in the scenario without C(s), apparently present the best performances, since Figures 4(b) and 5(b) are the only graphs to present significant amounts of ethane, albeit in smaller molar fractions, than expected by analyzing typical patterns of incipient defects. A more detailed evaluation of these two systems reveals that System 3 is probably better suited to represent the OMI decomposition than System 2, given that the latter 4 (b) presents a abrupt compositional change around the equilibrium temperature of 300 °C. Such an abrupt change is probably related to the absence of relevant species of intermediate molar masses in the system. As it is a more complete compositional model, System 3 allows a better representation of the range of decomposition products generated at specific temperatures.

It is also observed that, despite being developed based on compositional information, System 4 did not present, in this first qualitative analysis, the best performance when representing the thermal decomposition of the OMI. In addition to the absence of ethane in the entire temperature range studied, 5 (b) shows that methane is the only species of interest observed at equilibrium temperatures below 500°C, and also that the maximum amount of ethylene at equilibrium does not correspond to what is expected in typical patterns of defects incipient. Such observations are also valid for System 1, as shown in 2 (b).

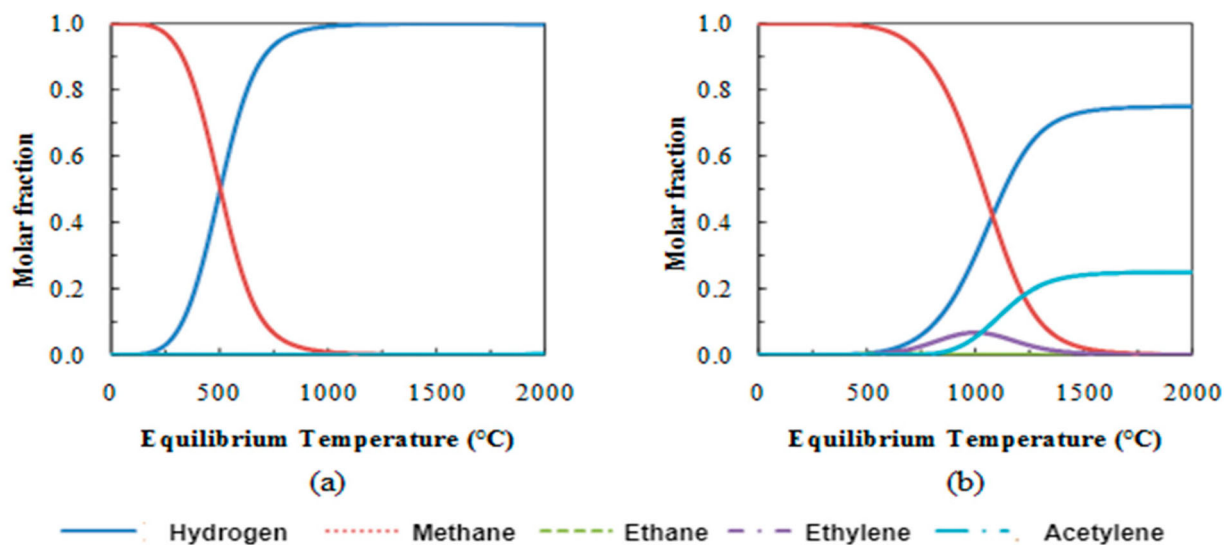


Figure 3. Normalized molar fractions of system 1 in equilibrium as a function of equilibrium temperature in two scales of C(s) size.

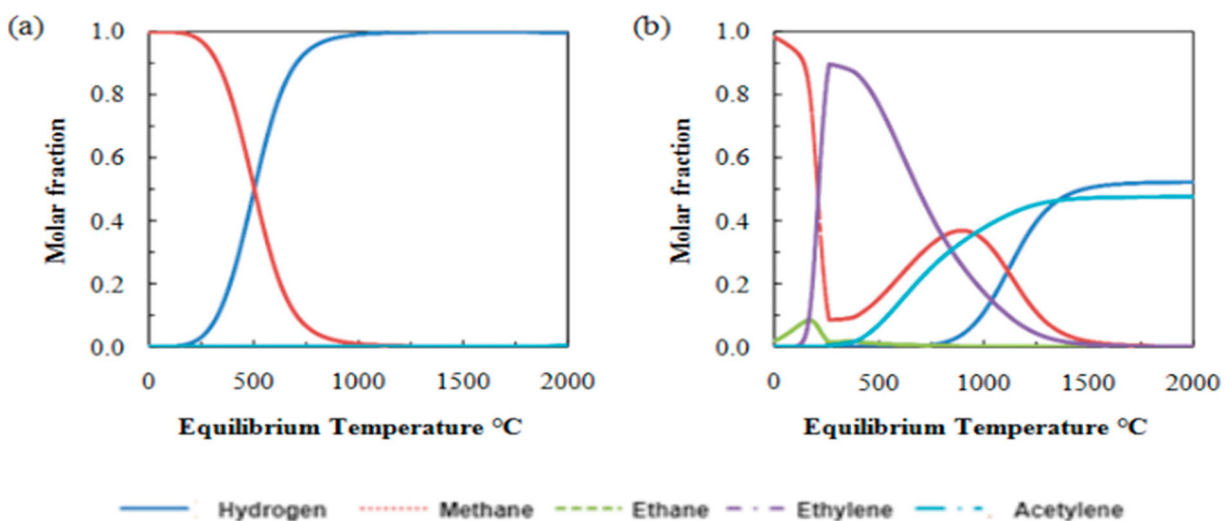


Figure 4. Normalized molar fractions of System 3 in equilibrium as a function of equilibrium temperature in two scenarios of amount of C(s). (a) – Scenario with unrestricted amount of C(s); (b) – Scenario without C(s).

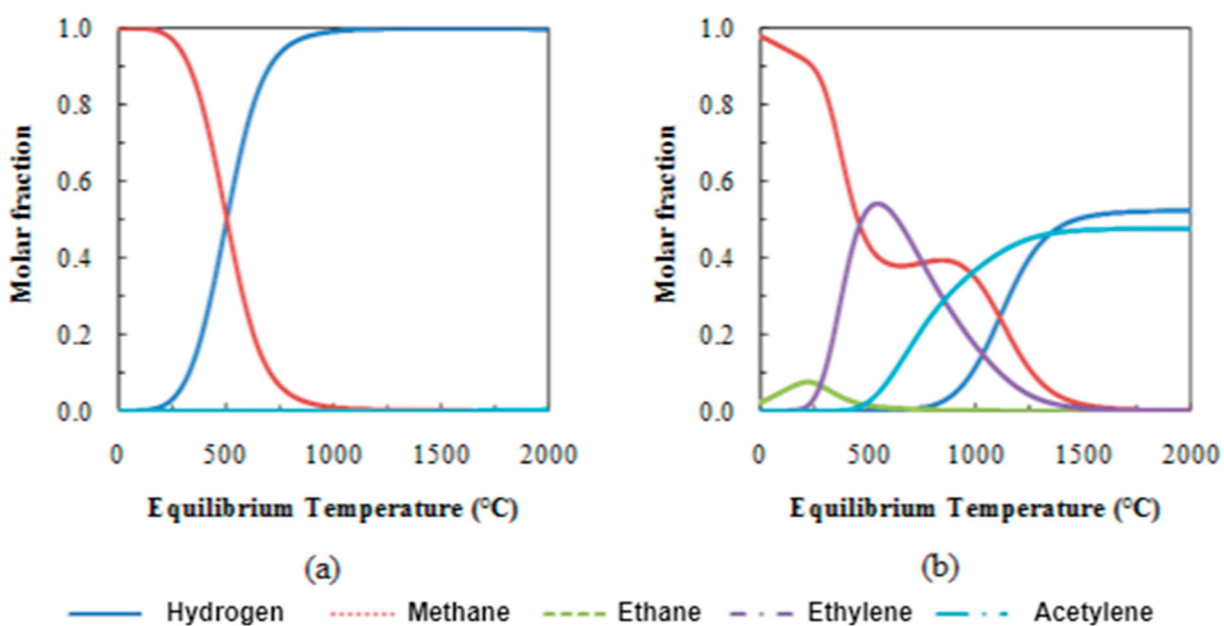
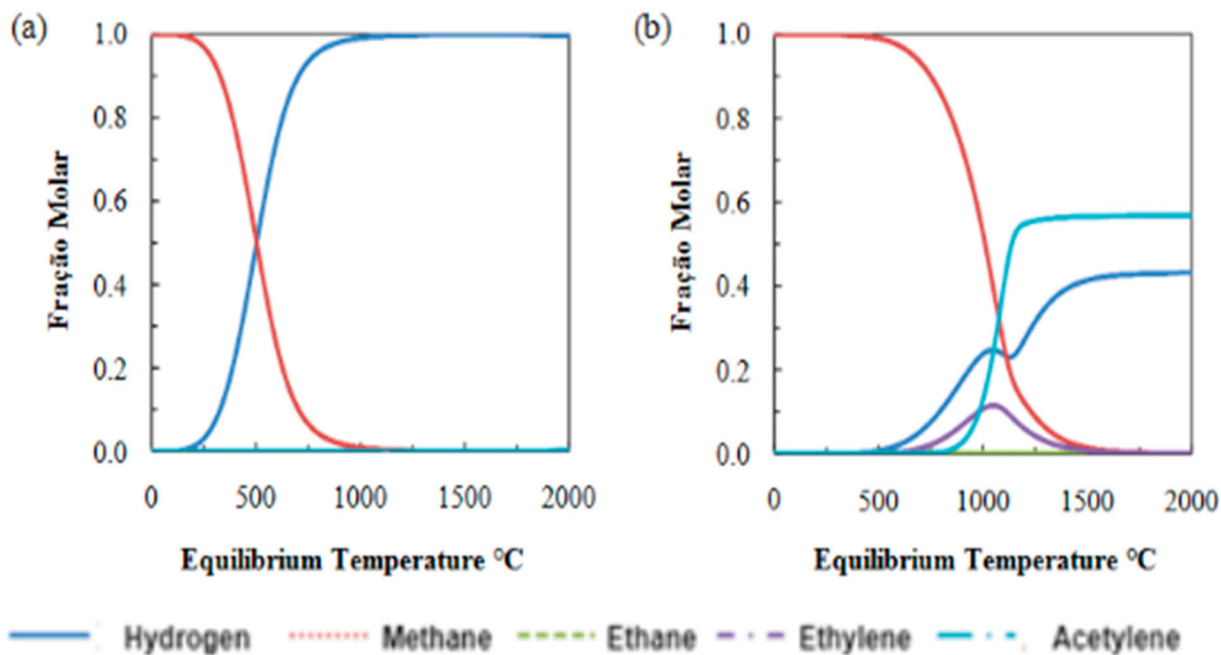


Figure 5. Normalized molar fractions of system 2 in equilibrium as a function of equilibrium temperature in two scales of C(s) size.



**Figure 6.** Normalized molar fractions of System 4 in equilibrium as a function of equilibrium temperature in two scenarios of amount of C(s). (a) – Scenario with unrestricted amount of C(s); (b) – Scenario without C(s).

### 5.3. Equilibrium molar fractions as a function of the amount of C(s)

The simulation is performed and the results are found with a model indicating the C(s) size for systems 1–4, respectively. The results were obtained at constant equilibrium temperature and the specified C(s) magnitude would vary from 0 to 1 based on the uncontrolled equilibrium area of C(s). Each simulation result is obtained for equilibrium temperatures of 0, 400, 800, 1200, 1600 and 2000 °C. Again, the figures cover only the molar fractions of the five types of interests for the purpose of comparison with the conventional forms of initial defects.

For all proposed compositional samples, the molar fractions of some species in the intermediate sequences of C(s) sizes differ significantly from those of the basic phenomena with C (the uncontrolled equilibrium magnitude of 0 and 100% indicating s.) Above the maximum temperature range studied. Therefore, the thermal decomposition of IMO is best represented in the intermediate displays of the C(s) magnitude, i.e. by the sample with the specification of the C(s) magnitude. In other words, the molar compounds derived from these intermediate scenarios may be more relevant than those derived from the absence of C(s), but with the advantage of presenting some amount of C(s) formation as empirical observations. It is also worth noting that at low temperatures, this behaviour is unique to System 2.

Molar fractions of interested species in all systems except ethane are highly sensitive to C(s) size variation at equilibrium temperature. In System 2 and 3, the variation of the molar fraction of hydrogen from zero to C(s) is found to be approximately 0.95, while C(s)

is uncontrolled. The molar fraction of hydrogen, as a function of the C(s) scales, in System 2 and 3, at certain temperatures, gives a pronounced non-monotonic behaviour.

Finally, the two systems exhibit similar behaviour at equilibrium, high temperature, consisting almost entirely of hydrogen and acetylene, whose molar fractions vary in line with the size of C(s). By analyzing the complete loops of the simulation results, such behaviour can be observed in both systems at temperatures above 1400 °C.

### 5.4. Performance evaluation of IMO thermal decomposition models

Table 1, Table 2 and Table 3 present descriptive statistical measures of the distribution of the optimal mean comparison errors calculated from the respective optimal values of the sum of the squares of comparison residues between the proposed models and the molar fractions and molar fractions coming from IEC database. Statistical measures that have provided grants for the quantitative evaluation of the performance of various proposed composite and thermodynamic equilibrium models. Tables refer to simulations in scenarios with optimal magnitudes of C(s) and C(s) without C(s), respectively.

By analyzing the data from the three tables, it can be observed that the reported optimal errors are generally higher. This is mainly due to the contribution of excess relative residues in cases with very small molar fractions in the IEC database. Nevertheless, as mentioned above, relatively high errors should be expected because

**Table 1.** Descriptive statistical measures of the distribution of the optimal mean relative errors representing a scenario with uncontrolled magnitude  $C(s)$ .

System	Average	Median	Standard deviation	90th percentile
System 1	8.74E + 08	92	8.20E + 09	642
System 2	8.72E + 08	92	8.17E + 09	642
System 3	8.71E + 08	92	8.15E + 09	642
System 4	8.71E + 08	92	8.15E + 09	642

**Table 2.** Descriptive statistical measures of the distribution of mean relative errors referring to the scenario without  $C(s)$ .

System	Average	Median	Standard deviation	90th percentile
System 1	2.03E + 11	81	2.18E + 12	1165
System 2	6.99E + 12	75	7.57E + 13	1948
System 3	8.29E + 12	76	9.70E + 13	1240
System 4	4.76E + 10	80	5.66E + 11	894

**Table 3.** Descriptive statistical measures of the distribution of mean relative errors referring to the scenario with optimized amount of  $C(s)$ .

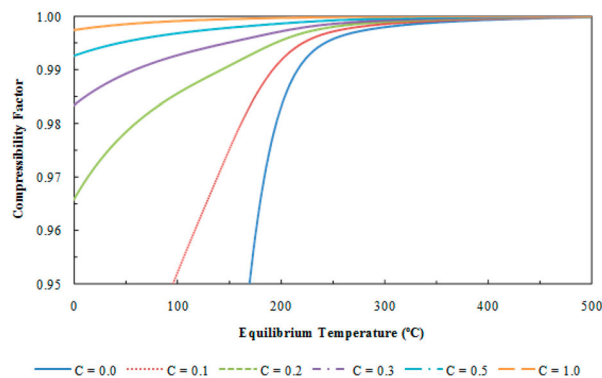
System	Average	Median	Standard deviation	90th percentile
System 1	94	65	107	135
System 2	66	56	45	75
System 3	73	57	60	85
System 4	79	58	85	101

empirical data are derived from operational equipment and not from planned tests.

The data in Table 1 confirm the simulated results provided, considering that the two proposed set models provided identical error operations. Measurements show that the errors associated with simulations are much higher in situations where the  $C(s)$  level is uncontrolled. Although the mean and the minimum are relatively small, the largest errors obtained have been proven to be the highest, as illustrated by the mean and the maximum. Even in the 90s, a measure that excludes the largest errors from the spread was shown to be high, indicating the occurrence of significantly higher errors.

Contrary to the reported expectations, the measurements given in Table 2 show that the errors associated with simulations in the absence of  $C(s)$  are generally higher than the errors in the situation with uncontrolled magnitude compared to the measurements given in Table 3.  $C(s)$ , indicated by very high mean and 90 percent values, although in some cases low errors were obtained, as revealed by the comparison of minima. Such observation reinforces the observation that although the Molar fraction profiles as a function of temperature are not intuitively derived from the quality rating, in fact both scales ( $s$ ) are poorly suited to model thermal decay. IMO.

As expected, Table 3 shows that an optimally sized display of  $C(s)$  leads to significantly lower average corresponding errors than those associated with other scenarios. Therefore, the proposed statistical measures

**Figure 7.** System 3 compressibility factors as a function of equilibrium temperature at constant fractions of the unrestricted equilibrium amount of  $C(s)$ .

confirm that controlling the  $C(s)$  level in the equation indicates an improvement in the IMO heat dissipation model. It should be noted that although the model with the optimal size  $C(s)$  introduces an additional parameter for problem solving, it also offers quality and fundamental improvements compared to the unrestricted size of the  $C(s)$  and  $C(s)$  equals zero, i.e. it gives equilibrium molar compounds comparable to conventional forms of initial defects and respects empirical observation of  $C(s)$  formation.

The data in Table 3 show that Systems 2 is the most adequate set of models with the most similar average error correlations to represent the IMO breakdown in the proposed models. The composite model of System 2, whose simulations provide very low average associated errors. Nevertheless, assuming that the small difference between the error distributions of System 2 may be the result of higher errors associated with the empirical data, and as a more complete set model, System 2 has more potential to adequately represent the error. IMO, moving forward from this point, decided to focus on the development of research on the chemical equilibrium of System 2.

### 5.5. Evaluating the validity of the ideal gas hypothesis

Figure 7 gives the estimated values for the compression factor of the system 3 equilibrium at different fractions of the constants  $C(s)$ ,  $C$ , and the latter, as a function of equilibrium temperature.

The best gas compression factor is approximately equal to one, and the best gas behaviour hypothesis is approximately valid for the closest compression factor. Therefore, it can be safely assumed that the correlation between the composite model proposed in IMO Thermal Decomposition Model 2 and the thermodynamic model that enhances the  $C(s)$  magnitude is valid for temperatures above 200°C for the full range of  $C$ . The validity of the hypothesis is that at low temperatures,  $C$  is greater than 0.2.

At low temperatures, it is not possible to distinguish the thermal decay of the IMO relative to the normal operating temperature of the transformer from the decay associated with the initial fault. Defective classification, very reasonable

### 5.6. Comparison between predicted and reported molar fractions

Figure 8 presents the optimal molar fractions predicted by System 3 with the optimal size of C(s) as a result of reducing the sum of the squares of comparative residues compared to the 117 cases in the IEC database. The diagrams show the optimal molar fractions as a function of the reported molar fractions for each type of interest. Corresponding types of initial defects are identified using different codes. Therefore, the IEC provides grants to assess the adequacy of the proposed model for the data, species of interest and type of defect.

Figure 8(a) refers that except for high-temperature thermal defects, the predicted hydrogen molar fractions show good agreement with the reported empirical data. Figure 8(b) indicates that the predicted methane molar fractions also showed good agreement with the reported data, however, in many cases the predicted values were higher than the reported data for thermal defects. Figure 8(c) indicates that the ethane molar fractions show little agreement with the reported data for all types of initial defects: all values predicted by the model were much lower than the reported experience data, which is consistent with the observed behaviour in practice Ethane molar fraction profiles. The ethylene molar fractions estimated in Figure 8(d) generally show some agreement with the reported data, although the model overestimates the molar fractions for thermal defects and underestimates the molar fractions for electrical faults. Figure 8(e) indicates that the predicted acetylene molar fractions with less than 0.45 molar fractions showed good agreement: for all data reported above this value, the sample predicts that the molar fractions will be close to 0.45. It is noteworthy that all the predictions, except for the predictions of acetylene molar fractions, showed poor agreement with the reported empirical data in the case of high-temperature thermal defects.

The relatively low compliance of predicted molar fractions with molar fractions in the IEC database is due not only to the errors associated with the modelling of the event, but also to the errors associated with the empirical database as already mentioned. In the case of acetylene in particular, it is noteworthy that the behaviour shown in Figure 8(e) is similar to that expected from the accumulation of dissolved gases over time in IMO, i.e. the empirical molar fractions may be higher time, reaching higher values than the maximum value predicted by the heat dissipation model.

### 5.7. Evaluation of results of the two-dimensional optimization problem

In order to expose the characteristics of the two-dimensional optimization problem, the Figure 9 presents the mean relative errors of randomly selected cases, grouped by their defect classifications, according to the IEC database, as a function of the percentage of the unrestricted amount of C(s). In each case, the temperature was kept constant at its optimum value.

It is possible to observe that the objective function can present different profiles, including the occurrence of local minima. Thus, the application of a brute force optimization method provided greater security in the identification of global minima, without, however, demanding a prohibitive computational effort, in view of the relatively small search intervals.

It is also interesting to note that the minimum error was not obtained in the scenario of unrestricted C(s) in any of these cases. In most cases, the minimum error was obtained in the intermediate scenario of amount of C(s), as expected., and, in some cases, the minimum error was obtained in the scenario with a quantity of C(s) equal to zero. Extending this analysis to all 117 cases presented in the IEC database, the optimization of the amount of C(s) resulted in smaller errors in 71.8% of the cases, when compared to the errors associated with scenarios with amounts of C(s) unrestricted or equal to zero. In the other 28.2% of the cases, the minimum errors were obtained in the scenario with a number of C(s) equal to zero. In none of the 117 cases, the minimum error was obtained in the scenario of unrestricted amount of C(s). As previously stated, the scenario with an unrestricted amount of C(s) leads to an equilibrium system where, essentially, only hydrogen and methane species are present, which, generally, does not reproduce the reported empirical data. For this reason, the scenario with an optimized amount of C(s) is a more suitable option compared to the scenario with an unrestricted amount of C(s), for all cases in the IEC database.

### 5.8. T-C diagnostic method

This section includes the results obtained in the stages of development of the phenomenologically based diagnostic method, the T-C method.

#### 5.8.1. Defect maps

Figure 10 shows the map of incipient faults, before being divided into regions, where DP means partial discharges, D1 means low energy electrical discharges, D2 means high energy electrical discharges, T1/T2 means low/medium temperature thermal defects and T3 means high-temperature thermal defects. This defect map was obtained from the adjustment, through

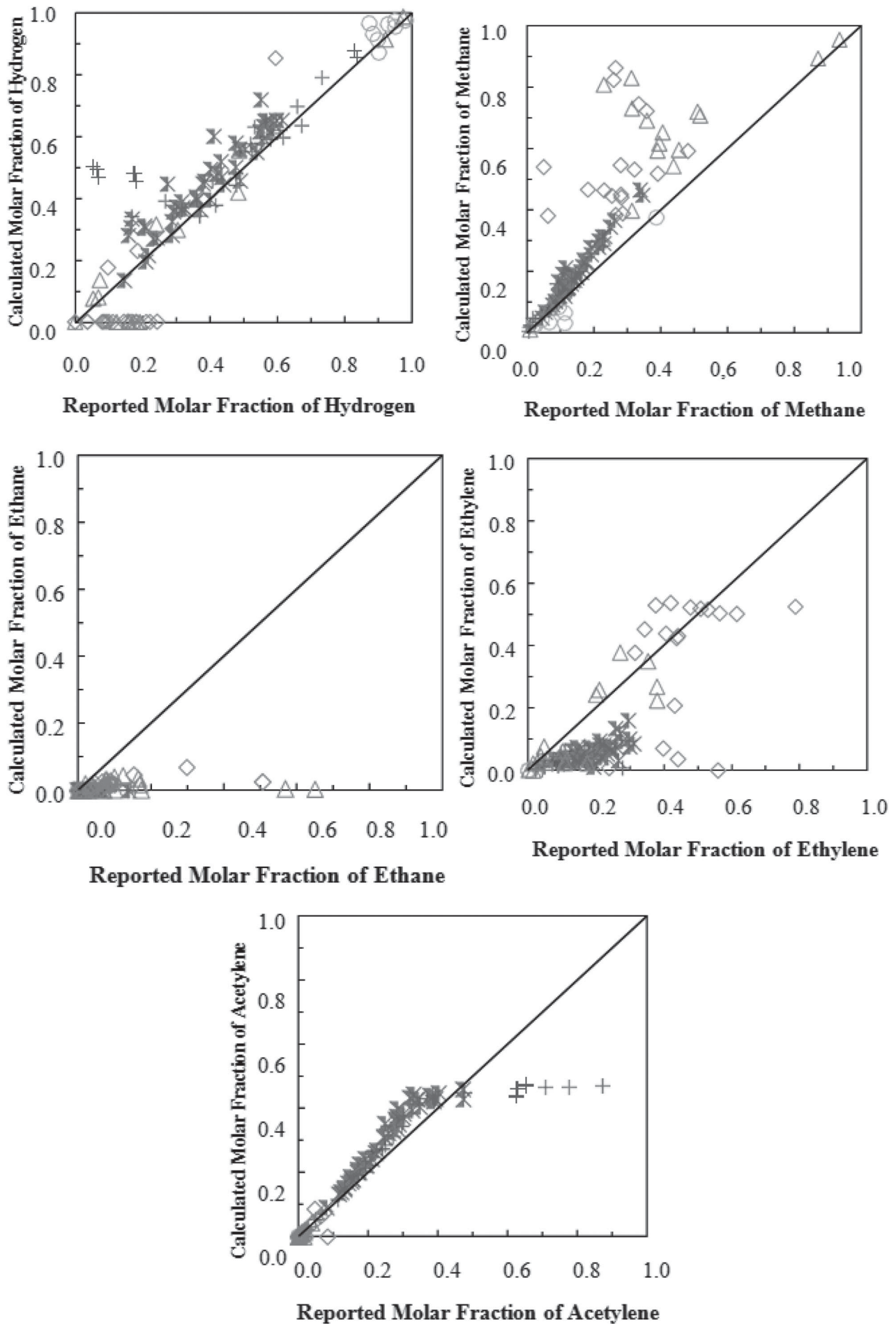


**Figure 8.** Predicted molar fractions versus reported molar fractions. (a) – Hydrogen; (b) – Methane; (c) – Ethane; (d) – Ethylene; (e) – Acetylene.

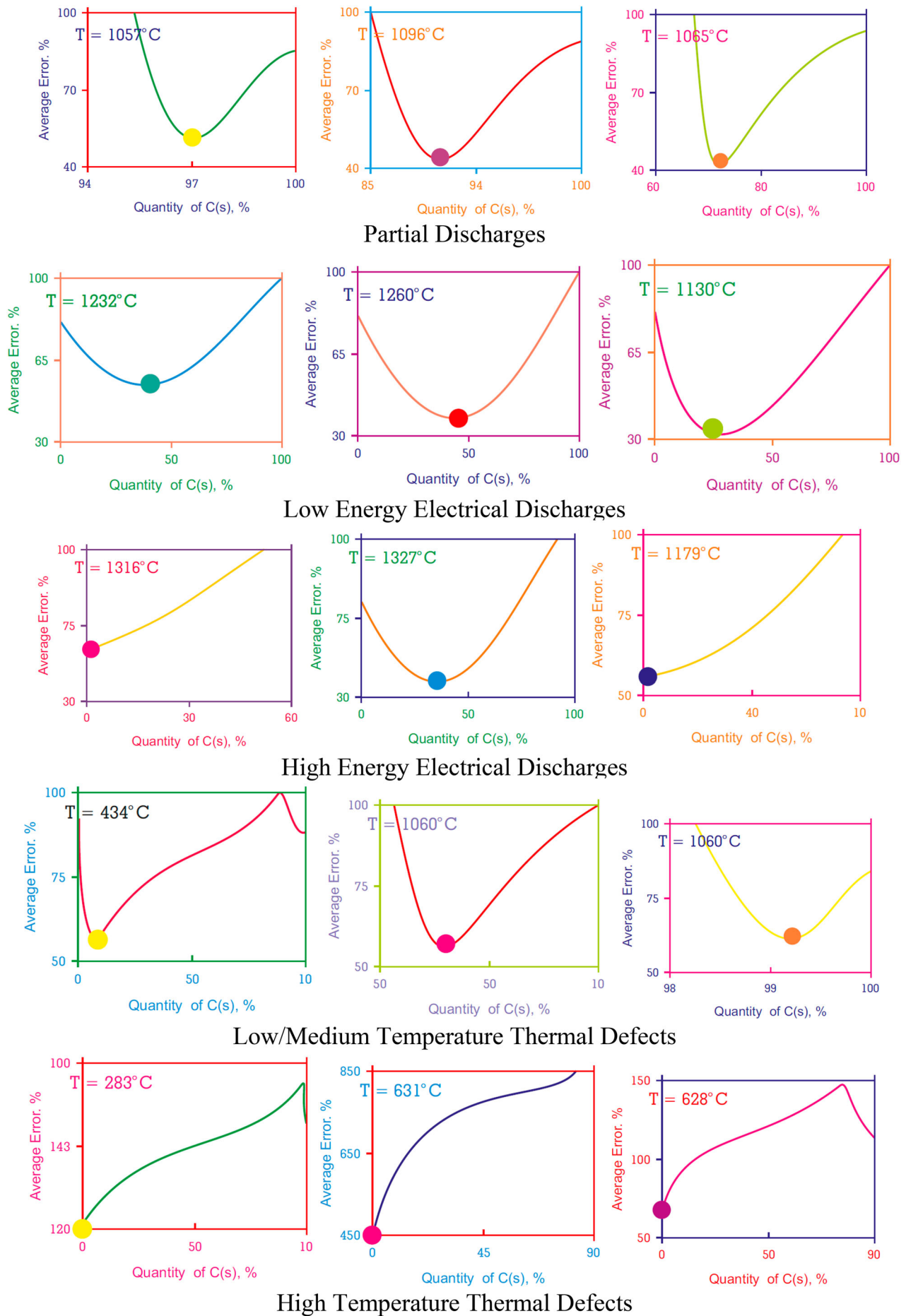
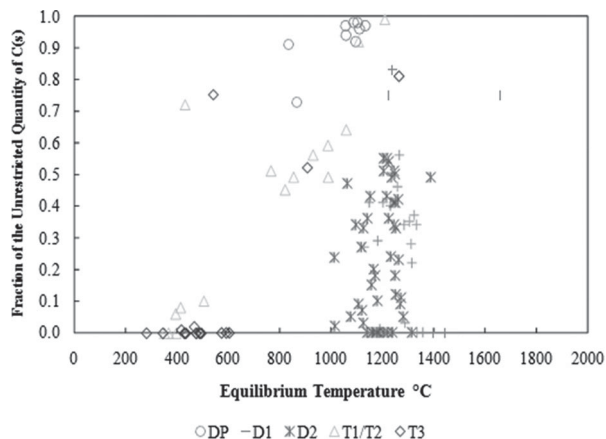


Figure 9. Mean relative errors as a function of the percentage of the unrestricted equilibrium amount of C(s) at constant temperature.



**Figure 10.** Map of incipient defects without subdivisions.

the solution of two-dimensional optimization problems, of the decomposition model to the 117 patterns of dissolved gases from the IEC database. It is worth mentioning that the decomposition model mentioned consists of the application of System 3 to the thermodynamic model with optimization of the amount of C(s). For the elaboration of the defect maps, the most refined hypermatrix of predicted molar fractions was used, that is, the hypermatrix with dimensions  $2001 \times 101 \times 5$ , with increments of 0.01 in the fraction of the unrestricted amount of equilibrium of C(s).

It is observed that the empirical data are well distributed in the graph and that the T-C binaries corresponding to the incipient defects of the DP types, thermal defects, DT (T1/T2 and T3), and electrical discharges, DE (D1 and D2), are grouped together, which indicates the potential of the proposed method to classify incipient defects by AGD. It is also observed that most of the partial discharge data were plotted in a region of the graph corresponding to high fractions of the unrestricted equilibrium amount of C(s), the thermal defects data were plotted in regions of low temperatures and the electrical discharges were plotted in regions of high temperatures, which qualitatively corroborates the characteristics of the defects (4,5).

A visual inspection of Figure 10 enabled the idealization of delimitations to separate the plotted data into 3 triangular regions, aiming at maximizing correct diagnoses of the T-C method: (i) The DP region corresponds to the triangle with vertices at (830; 1), (830; 0.6) and (1218; 1), (ii) the region of DT corresponds to the triangle with vertices at (1218;1), (250; 0) and (900; 0) and (iii) the region of DE corresponds to the triangle with vertices at (900; 0), (1570; 0) and (1218; 1). Furthermore, unlikely T-C binary regions, that is, low temperature-high fraction of C(s) and high temperature-low fraction of C(s), which correspond to theoretically unlikely patterns of dissolved gases, proved to be unpopulated and not provide defect classification. From these observations, Figure 11 presents

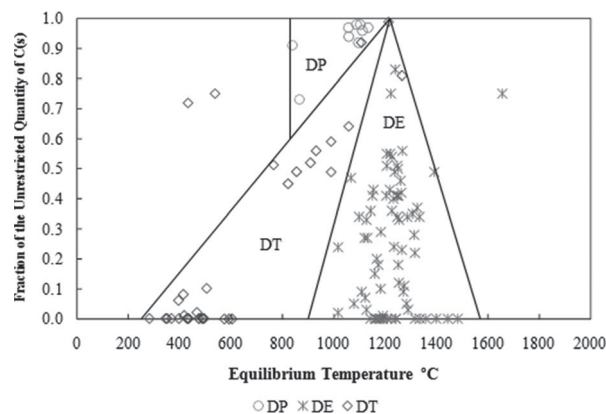


**Figure 11.** Map of incipient defects subdivided into three regions of defects.

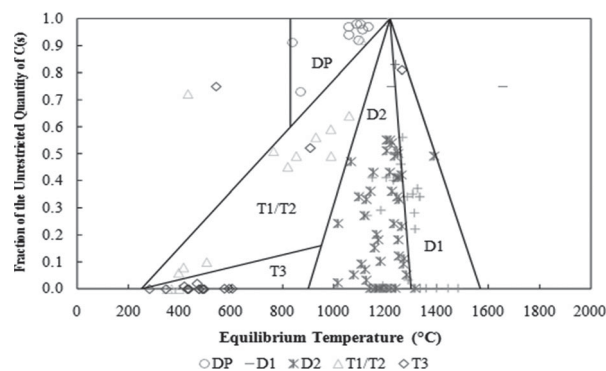


**Figure 12.** Map of incipient defects subdivided into five regions of defects.

the map of incipient defects divided into DP, DT and DE regions.

Figure 11 shows the map of incipient defects divided into regions DP, T1/T2, T3, D1 and D2, according to the types of incipient defects listed in the IEC database. Again, the procedure for delimiting the regions on the map was performed aiming at maximizing the performance of the T-C method.

In Figure 12, the DT region of Figure 11 was subdivided into the T1/T2 and T3 regions by a straight line passing through the points (250; 0) and (950; 0.16). Likewise, region DE was subdivided into regions D1 and D2 by a straight line passing through points (1218; 1) and (1300; 0).

### 5.8.2. Performance analysis of the T-C method

Table 4 presents the percentages of correct diagnoses given by the T-C method and by the Rogers, Doernenburg, IEC and Duval methods, resulting from the classification of cases in the IEC database into the three types of defects in the less refined division.

As seen in Table 4, the T-C method presented a much superior performance, in the classification in three regions, compared to the performance of the three classic methods based on ratios: Rogers, Doernenburg and IEC. In comparison to the Duval method, the T-C

**Table 4.** Performance of methods in classifying into three types of defects.

Diagnostic method	Correct diagnoses (%)
T-C (proposed method)	96
Rogers	57
Doernenburg	63
IEC	76
Duval	99

**Table 5.** Performance of methods in classifying into five types of defects.

Diagnostic method	Correct diagnoses (%)
T-C (proposed method)	80
Rogers	53
Doernenburg	63
IEC	69
Duval	89

method presented a very close performance, although a little lower.

Table 5 presents the performance of the methods in classifying the cases in the IEC database into the five types of defects in the most refined division.

A generalized performance loss is seen in Table 5 compared to Table 4, as expected from a more refined classification. The inspection of Figure 12 reveals that the DE data could not be satisfactorily separated into D1 and D2, which certainly impacts the percentage of correct diagnoses. Such an observation may indicate that parameters other than temperature and fraction of the unrestricted equilibrium amount of C(s) are necessary for a more adequate separation of this type of defects.

In addition, the previously cited conservative standardization of diagnostic method responses has led to the relatively small differences between the 3-region and 5-region ranking performances observed for some of these methods. The most extreme case was observed for the Doernenburg method, for which the performance in the classifications in 3 and 5 regions is the same.

In both classifications, in 3 and in 5 regions, the performance of the Rogers, Doernenburg and IEC methods, the methods based on ratios, clearly showed inferior when compared to the Duval and T-C methods, not based on ratios. As the selection of reasons is based on the Halstead model (6), the performances presented may be an indication that the low agreement of this model with the empirical data impairs the quality of the diagnostic methods or that relevant information is lost during the transformation. of dissolved gas concentrations in ratios.

The Duval diagnostic method, in turn, presented the highest performances. However, it is an empirical method and, therefore, the quality of its predictions is limited to the quality and scope of the base empirical data. The Duval method does not identify regions of unknown or unclassified classification, which implies

that any set of dissolved gas concentrations will be classified as a defect, even a theoretically unlikely set. Furthermore, this method discards two dimensions of the problem, the concentrations of H<sub>2</sub> and C<sub>2</sub>H<sub>6</sub>, and it is possible that relevant information is lost in this process.

On the other hand, the T-C diagnostic method is based on more adequate thermodynamic and compositional equilibrium models, when compared to Halstead's, and all the information on dissolved gases provided is explored, considering that the method applies the concentrations of the 5 species of interest to calculate the corresponding T-C binaries. The phenomenological basis of the method makes it possible to establish useful inferences, namely: the regions, already described, corresponding to theoretically improbable concentrations of dissolved gases can be used to verify the validity of the results of a dissolved gas test, since valid data do not should be observed in these regions. Regarding performance, it should be noted that the results of the T-C method were negatively impacted by the lack of regions of multiple defects, given that the conservative criteria adopted benefited the diagnostic methods that present such regions. Still, the T-C method exhibited performance close to the performance of the Duval method. Finally, the procedure for applying the T-C method may seem more complex than those of the classical methods, but this issue is easily overcome if the T-C method is implemented through a computational routine or even a spreadsheet.

Finally, it is worth remembering that the IEC database was built from information from equipment in operation and the calculated standards are subject to intrinsic errors. Therefore, it is possible that some empirical data have been misclassified, which in turn would contribute to the incorrect location of some T-C binaries in the incipient defect maps and, ultimately, to a reduction in the performance of the proposed diagnostic method.

## 6. Conclusion

This work presented and evaluated various thermodynamic and compositional modelling proposals for the thermal decomposition of insulating mineral oil. A new diagnostic method for DGA, the TC method, was developed from a more appropriate model than the options in the literature, and was improved and evaluated with the contribution inspired by the dynamics of the thermal decomposition phenomenon of the mineral oil. The comparison between the new diagnostic method and the classic method was successfully conducted and led to discussions about the basic principles of these methods. The profiles of the molar fractions as a function of temperature, obtained from the equilibrium C(s) quantity scenarios available in the literature, show that, at initial evaluation, there is little agreement for the display with the uncontrolled magnitude of C(s).

Experimental data and a scenario with a C(s) equivalent to zero would have a high potential to adequately represent the thermal decomposition that protects the mineral oil. However, on subsequent quantitative evaluation, it was proved that both quantities of C(s) in equilibrium were not sufficient to represent the event. The heat dissipation model with the C(s) size specification, i.e. the equilibrium size of C(s) in addition to the temperature, could be modified according to two hypotheses in the literature to the extent of C(s) in equilibrium. Furthermore, the proposed model, in a particular way, made it possible to simulate intermediate scenes of equilibrium C(s) with the aim of taking into account the dynamics of the event. The two-dimensional simulation results obtained with this model showed greater agreement with the empirical data than those obtained from the classical models available in the literature.

### Acknowledgments

The authors extend their appreciation to the Deanship of Scientific Research at King Khalid University for funding this work through a Large Group Research Project under grant number: RGP 2/177/44.

### Disclosure statement

No potential conflict of interest was reported by the author(s).

### References

- [1] Yang Z, et al. Association rule mining-based dissolved gas analysis for fault diagnosis of power transformers. *IEEE Trans Syst Man Cybern C*. 2009;39(6):597–610. doi:10.1109/TSMCC.2009.2021989.
- [2] Sun H-C, et al. A review of dissolved gas analysis in power transformers. *Energy Procedia*. 2012;14:1220–1225. doi:10.1016/j.egypro.2011.12.1079.
- [3] Wani SA, et al. Smart diagnosis of incipient faults using dissolved gas analysis-based fault interpretation matrix (FIM). *Arab J Sci Eng*. 2019;44(8):6977–6985.
- [4] Zhang Y, et al. Power transformer fault diagnosis considering data imbalance and data set fusion. *High Voltage*. 2020;6(3):543–554.
- [5] Senoussaoui MEA. Contribution des techniques intelligentes au diagnostic industriel des transformateurs de puissance. Thesis, Université DJILLALI LIABBES DE SIDI BEL ABBES (2019).
- [6] Bustamante S, et al. Dissolved gas analysis equipment for online monitoring of transformer oil: A review. *Sensors*. 2019;19(19):4057.
- [7] Cheng L, Yu T. Dissolved gas analysis principle-based intelligent approaches to fault diagnosis and decision making for large oil-immersed power transformers: A survey. *Energies*. 2018;11(4):913.
- [8] Taecharoen P, Kunagonnuyomrattana P, Chotigo S. Development of dissolved gas analysis analyzing program using visual studio program. In: 2019 IEEE PES GTD grand international conference and exposition Asia (GTD Asia), pp. 785–790. IEEE (2019).
- [9] IEEE Guide for the Interpretation of Gases Generated in Mineral Oil Immersed Transformers. IEEE. 2019.
- [10] Duval M.. 1974. Fault gases formed in oil-filled breathing E.H.V. power transformers—The interpretation of gas analysis data. In *IEEE Transactions on Power Apparatus and Systems* (No. 6, pp. 1745–1746). 345 E 47TH ST, NEW YORK, NY 10017-2394: IEEE-INST ELECTRICAL ELECTRONICS ENGINEERS INC.
- [11] Duval M, Lamarre L. The duval pentagon—A new complementary tool for the interpretation of dissolved gas analysis in transformers. *IEEE Electr Insul Mag*. 2014;30(6):9–12. doi:10.1109/MEI.2014.6943428.
- [12] Mansour D-EA. Development of a new graphical technique for dissolved gas analysis in power transformers based on the five combustible gases. *IEEE Trans Dielectr Electr Insul*. 2015;22(5):2507–2512. doi:10.1109/TDEI.2015.004999.
- [13] Gouda OE, El-Hoshy SH, El-Tamaly HH. Proposed heptagon graph for DGA interpretation of oil transformers. *IET Gener Transm Distrib*. 2018;12(2):490–498.
- [14] Gouda OE, El-Hoshy SH, El-Tamaly HH. Condition assessment of power transformers based on dissolved gas analysis. *IET Gener Transm Distrib*. 2019;13(12):2299–2310. doi:10.1049/iet-gtd.2018.6168.
- [15] IEEE Guide for the Detection and Determination of Generated Gases in Oil-Immersed Transformers and Their Relation to the Serviceability of the Equipment. ANSI/IEEE. 1978.
- [16] Rogers R. IEEE and IEC codes to interpret incipient faults in transformers, using gas in oil analysis. *IEEE Trans Electr Insul*. 1978;EI-13(5):349–354.
- [17] Interpretation of the analysis of gases in transformers and other Oil filled electrical equipment's in service. IEC Publication. 1999; 60599.
- [18] Gouda OE, El-Hoshy SH, El-Tamaly HH. Proposed three ratios technique for the interpretation of mineral oil transformers based dissolved gas analysis. *IET Gener Transm Distrib*. 2018;12(11):2650–2661.
- [19] Liang J-F, An J, Gao J-Q, et al. Identification of transformer fault based on dissolved gas analysis using hybrid support vector machine-modified evolutionary particle swarm optimisation. *PLoS One*. 2018;13(1):e0191999, doi:10.1371/journal.pone.0191999.
- [20] Nagpal T, Brar YS. Artificial neural network approaches for fault classification: Comparison and performance. *Neural Comput Appl*. 2014;25(7–8):1863–1870.
- [21] Ghoneim SSM, Taha IBM, Elkalashy NI. Integrated ANN-based proactive fault diagnostic scheme for power transformers using dissolved gas analysis. *IEEE Trans Dielectr Electr Insul*. 2016;23(3):1838–1845.
- [22] Yang X, et al. BA-PNN-based methods for power transformer fault diagnosis. *Adv Eng Inf*. 2019;39:178–185.
- [23] Du H, Wang G, Li J. Transformer fault identification with an IF1DCNN based on informative integration of heterogeneous sources. *Math Probl Eng*. 2021;2021:1.
- [24] Kari T, et al. Hybrid feature selection approach for power transformer fault diagnosis based on support vector machine and genetic algorithm. *IET Gener Transm Distrib*. 2018;12(21):5672–5680.
- [25] Abu-Siada A, Hmood S. A new fuzzy logic approach to identify power transformer criticality using dissolved gas-in-oil analysis. *Int J Electr Power Energy Syst*. 2015;67:401–408.
- [26] Noori M, Effatnejad R, Hajhosseini P. Using dissolved gas analysis results to detect and isolate the internal faults of power transformers by applying a fuzzy logic method. *IET Gener Transm Distrib*. 2017;11(10):2721–2729.

- [27] Poonnoy SN, Suwanasri CT. Fuzzy logic approach to dissolved gas analysis for power transformer failure index and fault identification. *Energies*. 2021; 14(1):36.
- [28] Shaaban S, Nabwey H. Transformer fault diagnosis method based on rough set and generalized distribution table. *Int J Intelligent Eng Syst*. 2012;5(2): 17–24.
- [29] Xue M. State evaluation for transformer based on grey system theory. *Appl Mech Mater*. 2014;488-489:983–987.
- [30] Mo W, et al. Power transformer fault diagnosis using support vector machine and particle swarm optimization. In: 2017 10th international symposium on computational intelligence and design (ISCID), pp. 511– 515. IEEE; 2017.
- [31] Cao Z, et al. Application of particle swarm optimization algorithm in power transformer fault diagnosis. *J Phys Conf Ser*. 2020;1624:042022.
- [32] Bartnikas R. *Engineering dielectrics*. Chelsea (MI): ASTM International; 1994; 8 v. V. 3: Electrical Insulating liquids.